

Supplementary information

Organic Heterojunction Charge-Transfer Chemical Sensors

Marc Courté,^{a*} Anderson Hoff,^b Gregory C. Welch,^b Loren G. Kaake^{a*}

^a Department of Chemistry, Simon Fraser University, Vancouver, British Columbia, Canada, V5A 1S6

^b Department of Chemistry, University of Calgary, 2500 University Drive N.W., Calgary, Alberta, Canada, T2N 1N4

Figure S1. I-V curve response of PDI-NH doped P(NDI2OD-2T) films	S2
Figure S2. I-V curve response of PDI-NH doped P(NDI2OD-2T) films after exposure to butylamine vapor	S2
Figure S3. Repeated response/recovery of the sensor exposed to n-butylamine vapor	S3
Figure S4: Stability performance of PDI-NH doped P(NDI2OD-2T) films	S3
Figure S5. Atomic Force spectroscopy (AFM) images of P(NDI2OD-2T) films	S4
Figure S6. Cadaverine sensitivity response of PDI-NH doped P(NDI2OD-2T) films	S4
Table S1. OFET characteristics	S5
Figure S7. Thickness measurement of a representative PDI-NH doped P(NDI2OD-2T) film	S5
Figure S8. UV-Visible spectra of PDI-NH doped P(NDI2OD-2T) films	S6
Figure S9. NOVEC 7100 sensitivity response of PDI-NH doped P(NDI2OD-2T) film	S6
Table S2. Comparison with recently reported ammonia/amine sensors	S7
Figure S10. UV-Vis of PDI-NH doped P(NDI2OD-2T) film treated with butylamine	S8
References	S9

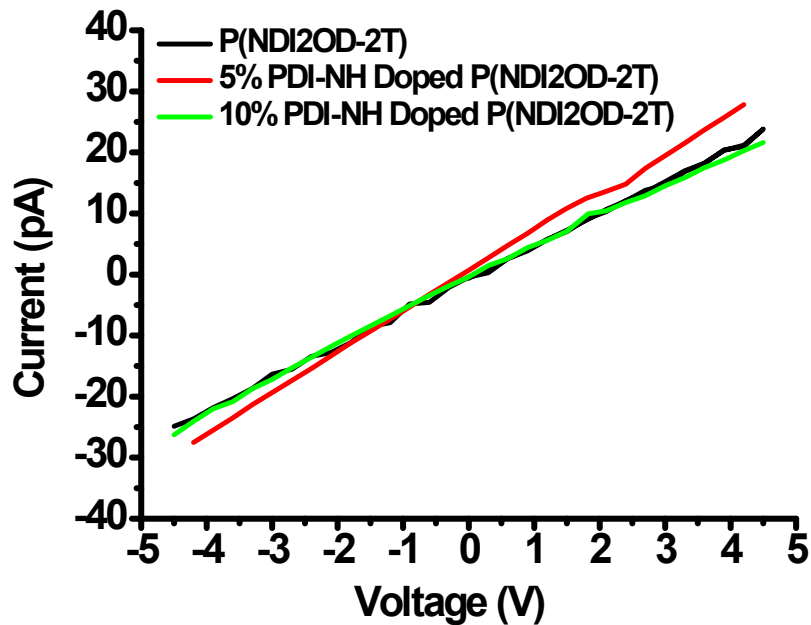


Figure S1. I-V curve response of P(NDI2OD-2T) films with different doping concentration in PDI-NH.

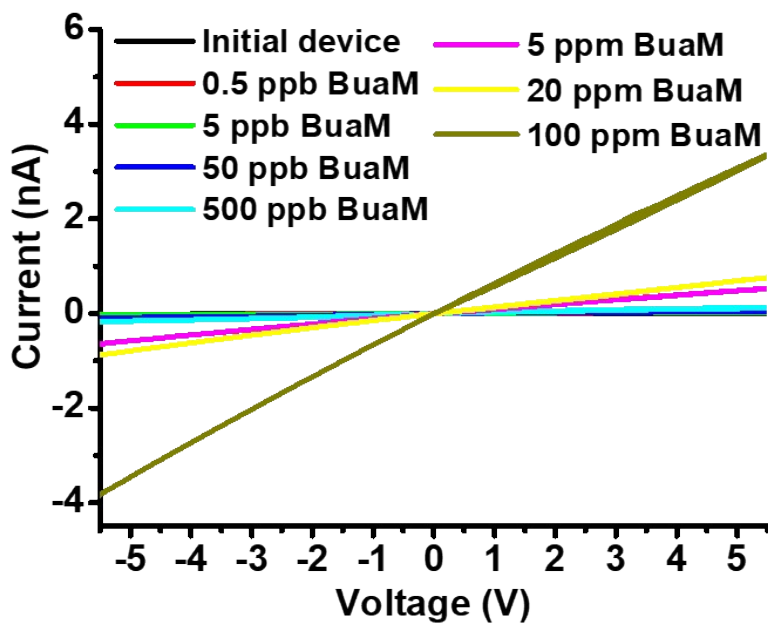


Figure S2. I-V curve response of P(NDI2OD-2T) films after exposure to different concentration (0.5 ppb – 100 ppm) of n-butylamine vapor.

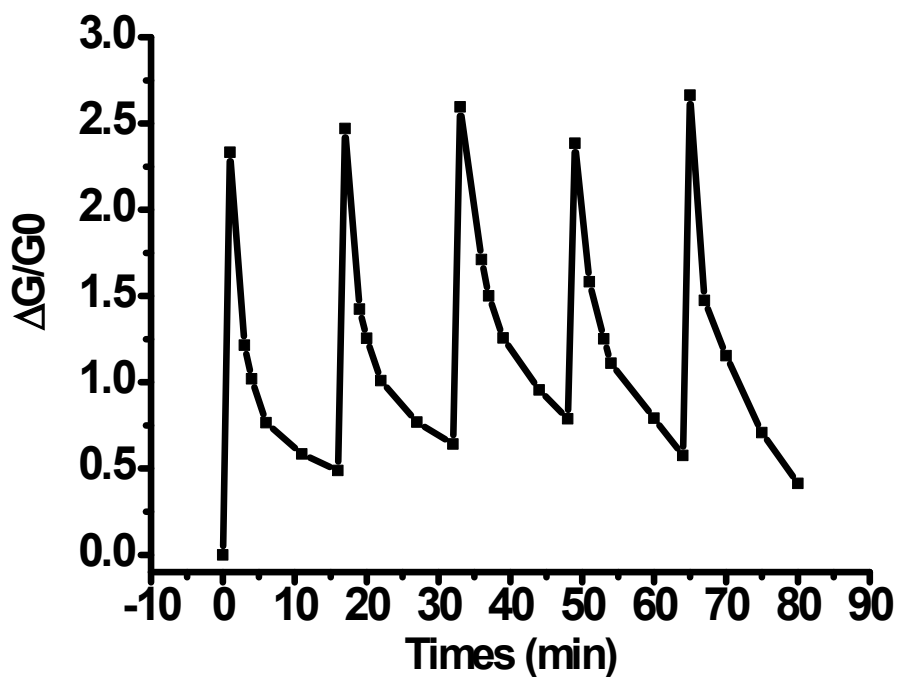


Figure S3. Repeated response/recovery of the PDI-NH doped P(NDI2OD-2T) film exposed to 0.5 ppm of n-butylamine.

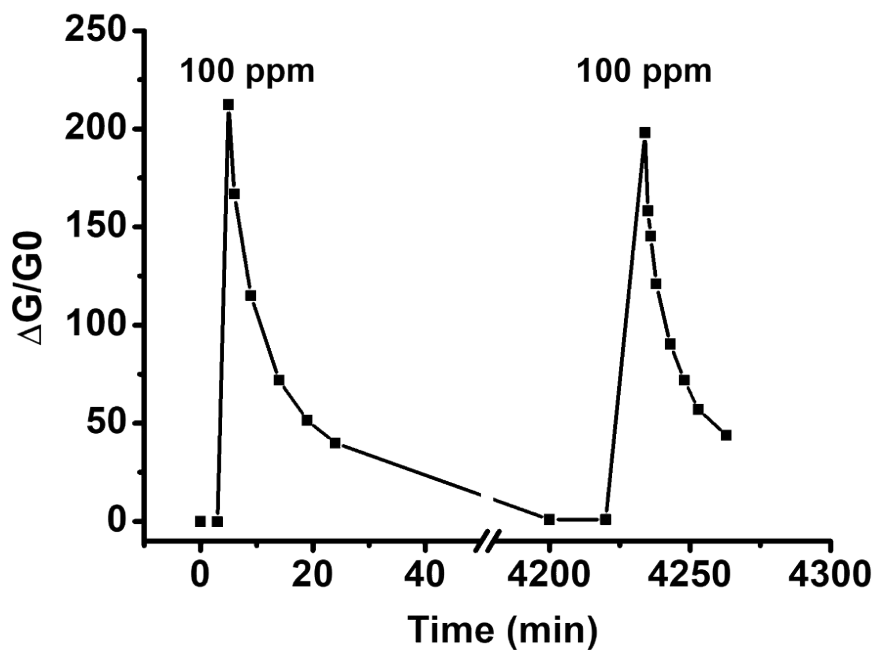


Figure S4: Stability performance of the PDI-NH doped P(NDI2OD-2T) film over days when exposed to 100 ppm of n-butylamine

P(NDI2OD-2T)

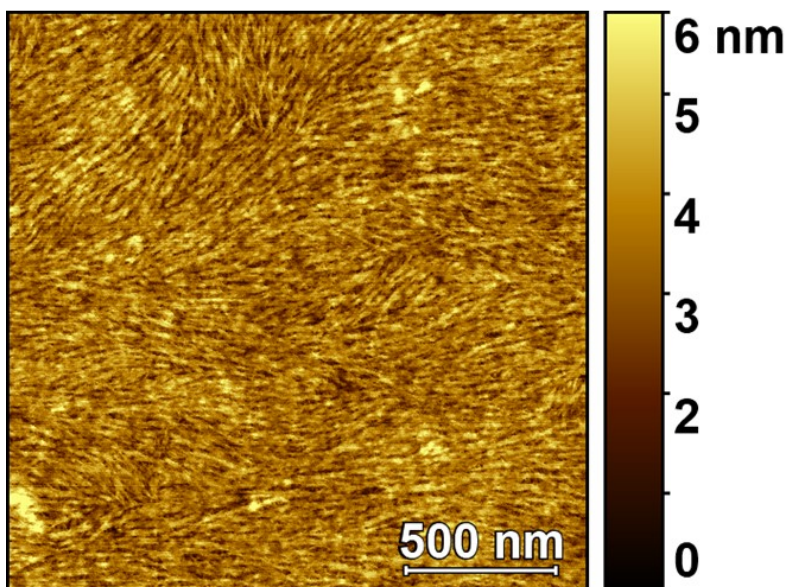


Figure S5. Atomic Force spectroscopy (AFM) images ($2\ \mu\text{m} \times 2\ \mu\text{m}$) of P(NDI2OD-2T) films deposited by spin-coating on glass substrates.

Cadaverine

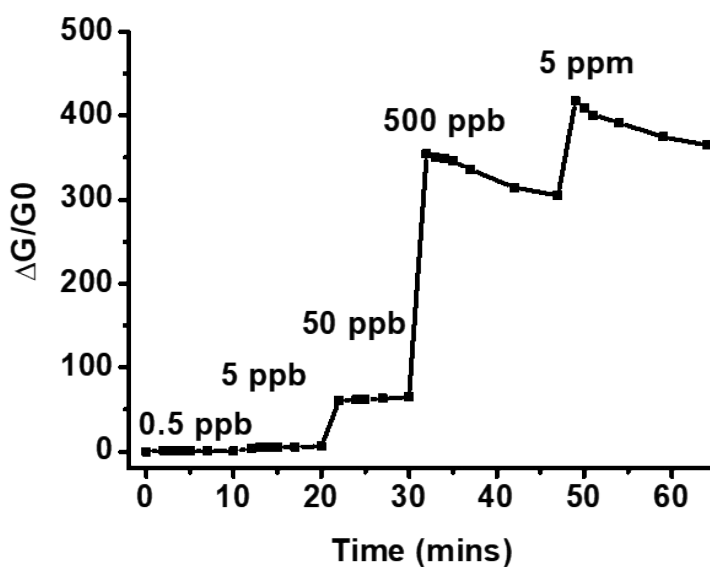


Figure S6. Sensitivity response of PDI-NH doped P(NDI2OD-2T) film after exposure to different concentration (0.5 ppb – 5 ppm) of cadaverine.

Table S1. Summary of the different OFET characteristics of PDI-NH doped P(NDI2OD-2T) film before and after exposure to Butylamine vapor

Samples	Before exposure to 5 ppm Butylamine			After exposure to 5 ppm Butylamine		
	Electron mobility $\text{cm}^2/(\text{V}\cdot\text{s})$	Threshold Voltage (V)	On/Off ratio	Electron mobility $\text{cm}^2/(\text{V}\cdot\text{s})$	Threshold Voltage (V)	On/Off ratio
N2200	0.005	21.2	4.0×10^4	0.007	1.3	$4. \times 10^4$
PDI-NH doped N2200	0.008	8.6	$2.8. \times 10^5$	0.01	-2.0	6.1×10^4

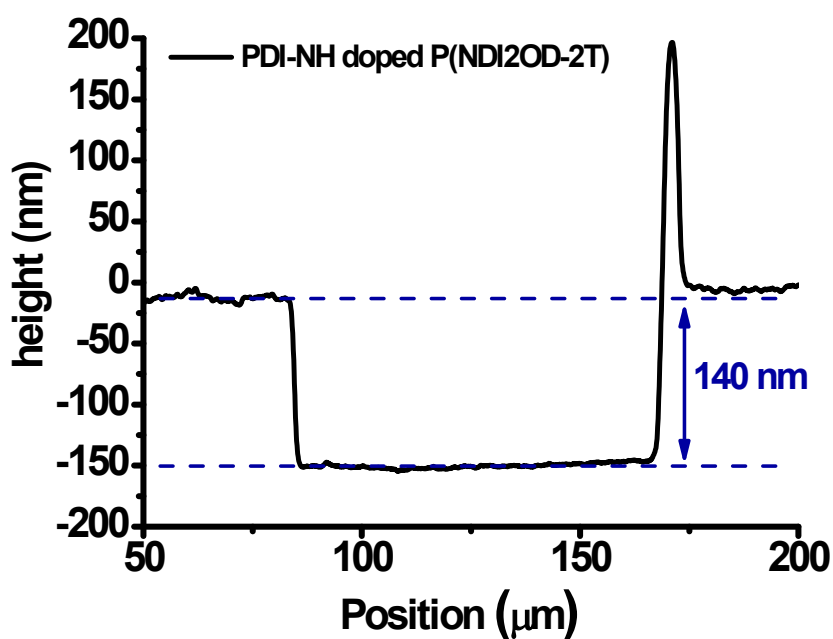


Figure S7. Profilometry thickness measurement of PDI-NH doped P(NDI2OD-2T) film deposited by spin-coating on a glass substrate.

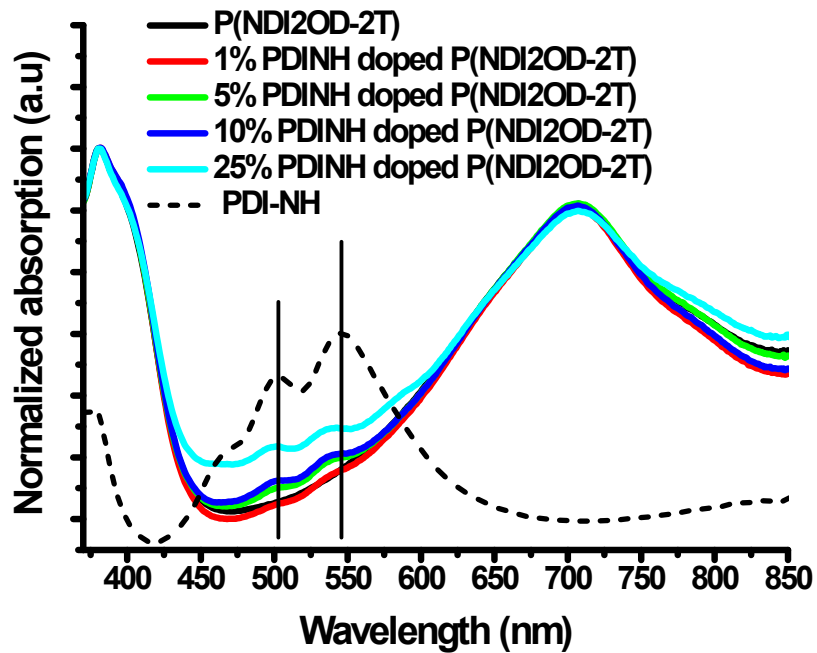


Figure S8. UV-Vis spectra of PDI-NH doped P(NDI2OD-2T) films for various doping concentration (straight line) and pristine PDI-NH (dot line) deposited by spin-coating on a glass substrate.

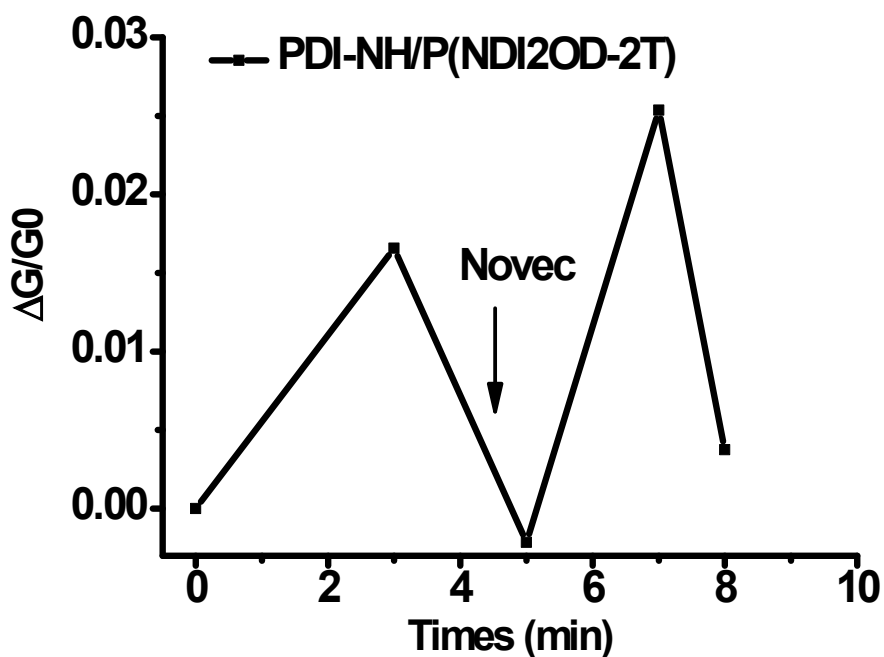


Figure S9. Sensitivity response of PDI-NH doped P(NDI2OD-2T) film after exposure to 0.5 mL of NOVEC.

Table S2. Comparison with recently reported ammonia/amine sensors.

Sensing material	Configuration/type	Analyte	Concentration in analyte	Sensing response (%)	Ref.
Our work	Chemiresistor	Butylamine	5 ppm	3 670	
		Cadaverine	5 ppm	66 500	
WO ₃ -SnO ₂	Chemiresistor	Ammonia	400 ppm	3 500	1
ZnO/PANI	Chemiresistor	Ammonia	10 ppm	2 150	2
		Butylamine	10 ppm	30	
PANI	Chemiresistor	Ammonia	10 ppm	220	2
SnO ₂ /ZnO NW	Chemiresistor	Butylamine	10 ppm	720	3
Sensitized TiO ₂	Chemiresistor	Methylamine	10 ppm	11.3	4
Pd decorated ZnO	Chemiresistor	Methylamine	100 ppm	99.5	5
{SiO ₂ :ZnO/3,5-dinitrophenyls}	Chemiresistor	Butylamine	50 ppm	90	6
SWCNTs metalloporphyrin	Chemiresistor	Ammonia	5 ppm	4	7
		Cadaverine	2.5 ppm	10	
		Putrescine	2.5 ppm	10	
PDI-HIS	Chemiresistor	Ammonia	50 ppm	1 700	8
PTTEH	OFET	Ammonia	10 ppm	30	9
P3HT	Chemiresistor	Ammonia	500 ppb	34	10
		Dimethylamine	500 ppb	18	
		Trimethylamine	500 ppb	10	
Cu ₃ (HHTP) ₂ MOF	Chemiresistor	Ammonia	100 ppm	129	11
CuTHPP-MOF	Chemiresistor	Cadaverine	0.1 μL	10	12
NDI(2OD)(4tBuPh)-DTYM2	OFET	Ammonia	100 ppm	20	13
DTBDT-C6	OFET	Ammonia	10 ppm	30	14
PTS-Pani	Chemiresistor	Ammonia	5 ppm	225	15
		Cadaverine	5 ppm	46	
		Putrescine	5 ppm	17	
SWCNT-N-C6F4CO ₂ H	Chemiresistor	Ammonia	40 ppm	10.8	16
		Trimethylamine	40 ppm	9.3	
graphene-encased gold nanorod	Nanoplasmonic	Cadaverine	0.1 mM	100	17

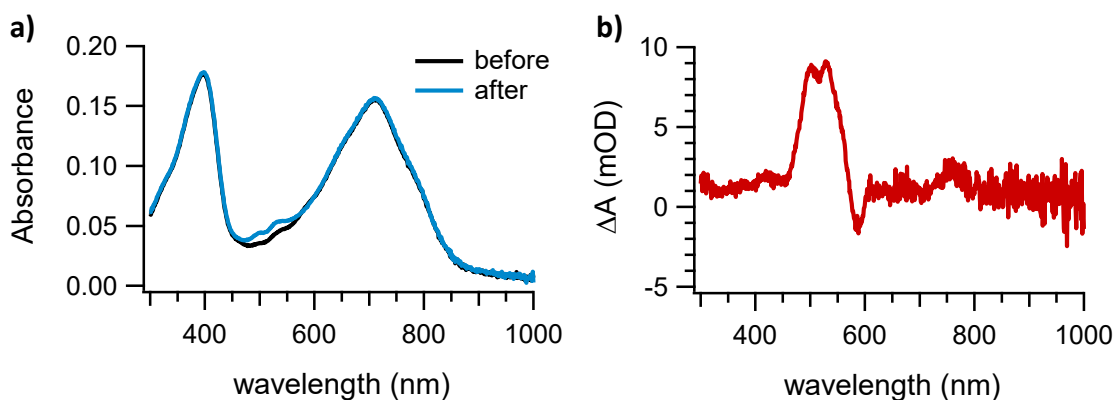


Figure S10. UV-Vis spectra of PDI-NH doped P(NDI2OD-2T) film treated with butylamine. a) before and after treatment with butylamine. b) calculated difference spectrum.

The absorbance spectra in fig. S10a are dominated by features associated P(NDI2OD-2T). Upon treatment with butylamine, a subtle increase in absorbance occurs around approximately 510 nm. Subtracting the spectrum before amine treatment from the spectrum after treatment yields the difference spectrum in S10b. Positive going features indicate species not in the spectrum before amine treatment. Most notable is a peak near 510 nm, consistent with electron transfer from the PDIN anion to P(NDI2OD-2T). The peak at 510 nm does not correspond to PDIN anion,¹⁸ but the singly charged anion of P(NDI2OD-2T).¹⁹ Additional structure from the bleached PDINH absorbance is superimposed on the P(NDI2OD-2T) anion. The bleach of neutral P(NDI2OD-2T) features is not clearly apparent, presumably because overlap with PDIN.

References

- 1 A. K. Nayak, R. Ghosh, S. Santra, P. K. Guha and D. Pradhan, *Nanoscale*, **2015**, 7, 12460–12473.
- 2 Y. Li, M. Jiao, H. Zhao and M. Yang, *Sensors and Actuators B: Chemical*, **2018**, 264, 285–295.
- 3 L. Wang, J. Li, Y. Wang, K. Yu, X. Tang, Y. Zhang, S. Wang and C. Wei, *Sci Rep*, **2016**, 6, 35079.
- 4 L. Yanxiao, Z. Xiao-bo, H. Xiao-wei, S. Ji-yong, Z. Jie-wen, M. Holmes and L. Hao, *Biosensors and Bioelectronics*, **2015**, 67, 35–41.
- 5 J. Bruce, K. Bosnick and E. Kamali Heidari, *Sensors and Actuators B: Chemical*, **2022**, 355, 131316.
- 6 R. S. Andre, Q. P. Ngo, L. Fugikawa-Santos, D. S. Correa and T. M. Swager, *ACS Sens.*, **2021**, 6, 2457–2464.
- 7 S. F. Liu, A. R. Petty, G. T. Sazama and T. M. Swager, *Angewandte Chemie International Edition*, **2015**, 54, 6554–6557.
- 8 A. Kalita, S. Hussain, A. H. Malik, N. V. V. Subbarao and P. K. Iyer, *J. Mater. Chem. C*, **2015**, 3, 10767–10774.
- 9 Z. Wang, Z. Liu, L. Chen, Y. Yang, J. Ma, X. Zhang, Y. Guo, G. Zhang and D. Zhang, *Advanced Electronic Materials*, **2018**, 4, 1800025.
- 10 L.-Y. Chang, M.-Y. Chuang, H.-W. Zan, H.-F. Meng, C.-J. Lu, P.-H. Yeh and J.-N. Chen, *ACS Sens.*, **2017**, 2, 531–539.
- 11 M.-S. Yao, X.-J. Lv, Z.-H. Fu, W.-H. Li, W.-H. Deng, G.-D. Wu and G. Xu, *Angewandte Chemie International Edition*, **2017**, 56, 16510–16514.
- 12 S. Zhang, L. Li, Y. Lu, J. Zhang, D. Liu, D. Hao, X. Zhang, L. Tian, L. Xiong and J. Huang, *J. Mater. Chem. C*, **2022**, 10, 5497–5504.
- 13 F. Zhang, C. Di, N. Berdunov, Y. Hu, Y. Hu, X. Gao, Q. Meng, H. Siringhaus and D. Zhu, *Advanced Materials*, **2013**, 25, 1401–1407.
- 14 L. Li, P. Gao, M. Baumgarten, K. Müllen, N. Lu, H. Fuchs and L. Chi, *Advanced Materials*, **2013**, 25, 3419–3425.
- 15 Z. Ma, P. Chen, W. Cheng, K. Yan, L. Pan, Y. Shi and G. Yu, *Nano Lett.*, **2018**, 18, 4570–4575.
- 16 C. Paoletti, M. He, P. Salvo, B. Melai, N. Calisi, M. Mannini, B. Cortigiani, F. G. Bellagambi, T. M. Swager, F. Di Francesco and A. Pucci, *RSC Adv.*, **2018**, 8, 5578–5585.
- 17 K. H. Kim, S. Jo, S. E. Seo, J. Kim, D.-S. Lee, S. Joo, J. Lee, H. S. Song, H. G. Lee and O. S. Kwon, *ACS Sens.*, **2023**, 8, 2169–2178.
- 18 C. R. Harding, J. Cann, A. Laventure, M. Sadeghianlemraski, M. Abd-Ellah, K. R. Rao, B. S. Gelfand, H. Aziz, L. Kaake, C. Risko and G. C. Welch, *Materials Horizons*, **2020**, 7, 2959–2969.
- 19 D. Trefz, A. Ruff, R. Tkachoy, M. Wieland, M. Goll, A. Kiriya and S. Ludwigs, *J. Phys. Chem. C*, **2015**, 119, 22760–22771.